PERFORMANCE EVALUATION OF HAMILTONIAN ENERGY CONTROL OF MULTIPHASE INTERLEAVED BOOST CONVERTER FOR FUEL CELL APPLICATIONS

[1]PONGSIRI MUNGPORN, [2]PHATIPHAT THOUNTHONG, [3]BABAK NAHID-MOBARAKEH, [4]NICU BIZON, [5]POOM KUMAM

[1,2]Renewable Energy Research Centre (RERC)
[2]Dept. Teacher Training in Electrical Engineering, Faculty of Technical Education
[1]Thai-French Innovation Institute 1518, Pracharat 1 Rd., Bangsue, Bangkok 10800, Thailand
[3]Serge Pierfederici, Damien Guilbert, GREEN Lab., LEMTA Lab., Université de Lorraine Avenue de la Forêt de Haye, 54504 Vandoeuvre les Nancy, France
[4]Faculty of Electronics, Communication, and Computers, University of Pitesti, Pitesti 110040, Romania
[5]Center of Excellence in Theoretical and Computational Science (TaCS-CoE), Science Laboratory Building, Faculty of Science, King Mongkut's University of Technology Thonburi (KMUTT), 126 Pracha-Uthit Road, Bang Mod, Thrung Khru, Bangkok 10140, Thailand
E-mail: [1]phatiphat.t@ieee.org, [2]phatiphat.t@fte.kmutnb.ac.th

Abstract - This paper studys a multi-phase boost fuel cell (FC) converter for dc microgrid applications. An original control law based on the Hamiltonian energy control principle for dc microgrid is considered. Using the port-controlled Hamiltonian property, we propose simple solutions to the system performance and stabilization problems when the interaction between power sources and constant power loads (CPLs). To corroborate the proposed control law, a prototype FC power converter (2.5-kW two-phase boost converter) is implemented in the laboratory. The Methanol FC system includes a fuel reformer that converts methanol and water liquid fuel into hydrogen gas to polymer electrolyte membrane FC (PEMFC) stack (2.5-kW, 50 V). The proposed control approach is realized with a digital estimate in a dSPACE MicroLabBox controller card. The experimental and simulation results verify that this is a good control scheme during constant power load cycles.

Keywords - Constant power load (CPL), dc microgrid, interleaved boost converter, interconnection and damping assignment (IDA), fuel cell (FC), passivity based controller (PBC), Port-Controlled Hamiltonian (PCH)

I. INTRODUCTION

Currently, fuel cell (FC) development and research have received much attention for their higher energy conversion efficiency and lower or nongreen house gas emissions than thermal engines in the processes of converting fuel into usable energies [1]–[3]. For the past fifteen years, much research has been conducted on the uses of FCs in high power applications. At present, the required FC power is in the scale of 1 kW to 1 MW [4]: 40–700 kW for manned aircraft; and 50–100 kW for urban cars.

Usually, an FC system needs a boost dc/dc converter (step-up converter) to adapt the FC output voltage to the desired dc bus voltage stage and smooth the FC current [5], [6], see Fig. 1. However, a single converter will be limited by many factors when the load power increases or for higher voltage step-up ratios. That way, the employ of paralleling

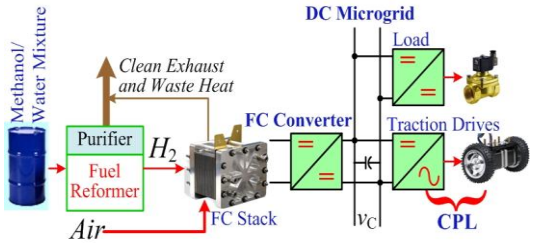


Fig. 1. DC microgrid supplied by a FC power source.

dc/dc power circuits with the interleaved technique may offer improved performance [7]. In this paper, we propose a multiphase dc/dc converters, which are connected at the output of the FC stack . The number of parallel converter modules N (with interleaving switching technique) would depend upon the rated power of the stack.

Nevertheless, it is recognized that CPLs in power systems may cause instability [8], [9]. In reality, when the load power is constant (example: a tightly regulated inverter-motor drive), the average load current i_{Load} absorbed by the load is equal to the load power over the dc link voltage ($i_{Load} = p_{Load}/v_C$). Therefore, when the voltage is regulated at a set-point or it may be small decreases, the load current inceases as though the CPL has a "negative impedance" = $-\Delta v_C/\Delta i_{Load}$ effect on the dc grid. The negative incremental impedance property of a CPL might cause a dc-grid voltage oscillation or even instability when classic linear controllers are utilized [10]. Much research effort has been dedicated to studying nonlinear control approaches for power converters with CPLs [11].

This paper presents the original control method based on the port-Controlled Hamiltonian theory for the multiphase FC power converter for dc microgrid applications. It will provide a significant contribution to the field of the power system, particularly in nonlinear power electronics applications. In Section II,

the brief of the Hamiltonian energy control, the multiphase converter modeling, the control law, and system stability are presented in detail. In Section III, experimental and simulation results will show the system performance during CPL cycles. The summary and conclusions are presented in Section IV.

II. MODELING AND CONTROL

A. Brief of The Port-Hamiltonian Energy Control

First, consider the class of nonlinear port-controlled Hamiltonian systems [12], [13] described by following equation

$$\dot{\mathbf{x}} = [\mathbf{J} - \mathbf{R}] \cdot \frac{\partial \mathbf{H}(x)}{\partial x} + \mathbf{g}(x) \cdot \mathbf{u} + \xi \,, \; \mathbf{y} = \mathbf{g}^T(x) \frac{\partial \mathbf{H}(x)}{\partial x} \quad (1)$$

where u(t) $\in \mathbb{R}^m$ is the input control variable, x(t) $\in \mathbb{R}^n$ is the state varariable of the system, y(t) $\in \mathbb{R}^m$ is the output variable, J is the interconnection skew symmetric matrix ($J = -J^T$), R is the damping matrix or dissipation symmetric matrix (positive-definite matrix, $R = R^T \geq 0$), H(x) is the Hamiltonian function (or energy function) and also known as a Lyapunov function, g(x) represents the port characteristic matrix of the plant, and ξ(t) is the input or disturbance variable. With the aforementioned conditions, it is essential to state that the dynamical system given by (1) is a passive dynamical system or passivity system [14], [15].

The idea of the Hamiltonian energy control (or known as the interconnection and damping assignment passivity-based control, IDA-PBC) design consists in determining a control input u such that a desired equilibrium point (fixed-point) x_d of the closed-loop system is (asymptotically) stable (see Fig. 1) and that the closed-loop system is described by the equations.

$$\dot{\mathbf{x}} = [\mathbf{J}_d - \mathbf{R}_d] \cdot \frac{\partial \mathbf{H}_d(x)}{\partial x} \quad (2)$$

where J_d is the the desired interconnection matrix $J_d = -J_d^T$, R_d is the desired damping matrix or dissipation matrix $R_d = R_d^T \geq 0$, and H_d is the desired energy function.

An algebraic equation needs to be solved in order to achieve the controller, with the constraint of skew symmetry matrix J_d and positive-definite matrix R_d [16],

$$\overbrace{[\mathbf{J}_d - \mathbf{R}_d] \cdot \frac{\partial \mathbf{H}_d(x)}{\partial x}}^{Control\ Law} = \overbrace{[\mathbf{J} - \mathbf{R}] \cdot \frac{\partial \mathbf{H}(x)}{\partial x} + \mathbf{g}(x) \cdot \mathbf{u} + \xi}^{Plant} \quad (3)$$

Then, one obtains

$$\mathbf{u} = \left([\mathbf{J}_d - \mathbf{R}_d] \cdot \frac{\partial \mathbf{H}_d(x)}{\partial x} - [\mathbf{J} - \mathbf{R}] \cdot \frac{\partial \mathbf{H}(x)}{\partial x} - \xi \right) \cdot \mathbf{g}^{-1}(x) \quad (4)$$

B. Multiphase Interleaved Boost Converter Average Model

Fig. 2 displays the circuit of the proposed multiphase interleaved boost converter for FC applications.

The differential equations of the multiphase converters are given as [17], [18]

$$\frac{d i_{LK}}{dt} = \frac{v_{FC}}{L_K} - \frac{R_K}{L_K} i_{LK} - \frac{(1 - d_K)}{L_K} v_C \quad (5)$$

$$\frac{d v_C}{dt} = \sum_{K=1}^{N} \left[\frac{(1 - d_K)}{C_{Bus}} i_{LK} \right] - \frac{i_{Load}}{C_{Bus}} \quad (6)$$

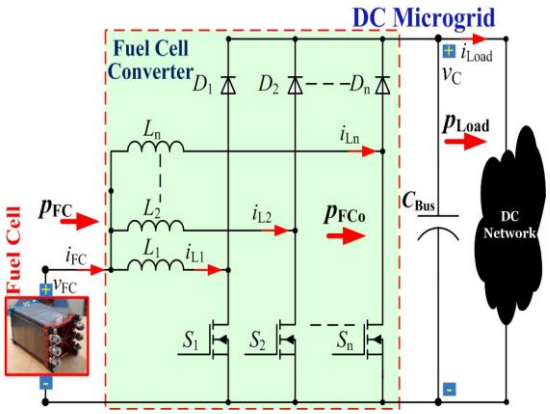


Fig. 2. Multiphase parallel interleaved boost converters for FC applications.

where the subscript number K = 1, 2, . . ., N represents the parameters of each converter module, v_C is the dc bus voltage, d_K is the duty cycle of the pulsewidth modulation (PWM) converter ($d_K \in [0,1]$), i_{FC} is the FC current, v_{FC} is the FC voltage, p_{FC} is the FC power ($= v_{FC} \cdot i_{FC}$), i_{LK} is the inductor current, i_{Load} is the load current at the dc bus, C_{Bus} is the total output capacitance at the dc bus, L is the input inductance, and R_K is the series resistance of inductor L_K. Note that R_K represents the static losses in each boost converter module.

Here, a 2-phase (N=2) boost converter is studied and implemented. One defines: the state variables $x = [x_1, x_2, x_3]^T = [i_{L1}, i_{L2}, v_C]^T$, and the control variables $u = [u_1, u_2]^T = [d_1, d_2]^T$. From the energy point of view, the Lyapunov energy function H(x) of the 2-phase boost converter with a CPL represents the total energy stored in the dynamic system and can be expressed as

$$\mathbf{H}(x) = \frac{1}{2} L_1 \cdot x_1^2 + \frac{1}{2} L_2 \cdot x_2^2 + \frac{1}{2} C_{Bus} \cdot x_3^2 \quad (7)$$

$$\frac{\partial \mathbf{H}(x)}{\partial x} = [L_1 x_1 \quad L_2 x_2 \quad C_{Bus} x_2]^T \quad (8)$$

Next, the converter model (5), (6), and (8) can be written in the Hamiltonian form (1)

$$\begin{bmatrix}\dot{x}_1\\ \dot{x}_2\\ \dot{x}_3\end{bmatrix}=\underbrace{\begin{bmatrix}-\frac{R_1}{L_1^2} & 0 & -\frac{1}{L_1C_{\text{Bus}}}\\ 0 & -\frac{R_2}{L_2^2} & -\frac{1}{L_2C_{\text{Bus}}}\\ \frac{1}{L_1C_{\text{Bus}}} & \frac{1}{L_2C_{\text{Bus}}} & 0\end{bmatrix}}_{\mathbf{J}-\mathbf{R}}\underbrace{\begin{bmatrix}L_1x_1\\ L_2x_2\\ C_{\text{Bus}}x_3\end{bmatrix}}_{\frac{\partial \mathbf{H}(x)}{\partial x}}+\underbrace{\begin{bmatrix}\frac{x_3}{L_1} & 0\\ 0 & \frac{x_3}{L_2}\\ -\frac{x_1}{C_{\text{Bus}}} & -\frac{x_2}{C_{\text{Bus}}}\end{bmatrix}}_{\mathbf{g}(x)}\underbrace{\begin{bmatrix}u_1\\ u_2\end{bmatrix}}_{\mathbf{u}}+\underbrace{\begin{bmatrix}\frac{v_{\text{FC}}}{L_1}\\ \frac{v_{\text{FC}}}{L_2}\\ \frac{i_{\text{Load}}}{C_{\text{Bus}}}\end{bmatrix}}_{\xi}$$

(9)

with,

$$\mathbf{J}=\begin{bmatrix}0 & 0 & -\frac{1}{L_1C_{\text{Bus}}}\\ 0 & 0 & -\frac{1}{L_2C_{\text{Bus}}}\\ \frac{1}{L_1C_{\text{Bus}}} & \frac{1}{L_2C_{\text{Bus}}} & 0\end{bmatrix},\ \mathbf{J}=-\mathbf{J}^T.$$

(10)

$$\mathbf{R}=\begin{bmatrix}\frac{R_1}{L_1^2} & 0 & 0\\ 0 & \frac{R_2}{L_2^2} & 0\\ 0 & 0 & 0\end{bmatrix},\mathbf{R}=\mathbf{R}^T\geq 0$$

(11)

C. Port-Controlled Hamiltonian System

Refer to (2) and (7), the desired Hamiltonian Lyapunov function is set as follows:

$$H_{\text{d}}(x)=\frac{1}{2}L_1\cdot(x_1-x_{1\text{d}})^2+\frac{1}{2}L_2\cdot(x_2-x_{2\text{d}})^2+\frac{1}{2}C_{\text{Bus}}\cdot(x_3-x_{3\text{d}})^2.$$

(12)

where x_{d} are the state variables. Then,

$$\frac{\partial H(x)}{\partial x}=\begin{bmatrix}L_1(x_1-x_{1\text{d}}) & L_2(x_2-x_{2\text{d}}) & C_{\text{Bus}}(x_3-x_{3\text{d}})\end{bmatrix}^T$$

. (13)

Then, we set J_{d} and R_{d} be of the same structure as the original J and R

$$\mathbf{J}_{\text{d}}=\mathbf{J}+\overbrace{\underbrace{\begin{bmatrix}0 & 0 & -K_{\text{j}13}\\ 0 & 0 & -K_{\text{j}23}\\ K_{\text{j}13} & K_{\text{j}23} & 0\end{bmatrix}}_{\text{Control Interconnection Matrix}}}^{J_C},\mathbf{J}_{\text{d}}=-\mathbf{J}_d^T$$

(14)

$$\mathbf{R}_{\text{d}}=\mathbf{R}+\overbrace{\underbrace{\begin{bmatrix}K_{\text{r}1} & 0 & 0\\ 0 & K_{\text{r}2} & 0\\ 0 & 0 & K_{\text{r}3}\end{bmatrix}}_{\text{Control Damping Matrix}}}^{R_C},\mathbf{R}_{\text{d}}=\mathbf{R}_{\text{d}}^{\text{T}}\geq 0$$

(15)

where J_c and R_c are the controller matrices. Refer to (4), the control law can be obtained as follows:

$$d_1=u_1=\frac{R_1i_{\text{L}1\text{d}}+K_{\text{r}1}L_1^2e_1+K_{\text{j}13}C_{\text{Bus}}L_1e_3+v_{\text{C}3\text{d}}-v_{\text{FC}}}{v_{\text{C}}}$$

(16)

$$d_2=u_2=\frac{R_2i_{\text{L}2\text{d}}+K_{\text{r}2}L_2^2e_2+K_{\text{j}23}C_{\text{Bus}}L_2e_3+v_{\text{C}3\text{d}}-v_{\text{FC}}}{v_{\text{C}}}$$

(17)

where the error variables $e_1 = i_{\text{L}1\text{d}} - i_{\text{L}1}$, $e_2 = i_{\text{L}2\text{d}} - i_{\text{L}2}$, and $e_3 = v_{\text{Cd}} - v_{\text{C}}$. $i_{\text{L}1\text{d}}$ and $i_{\text{L}2\text{d}}$ are the desired values of the boost converter inductance currents, and v_{Cd} is the desired output voltage for supplying the load. Towards this end, the desired inductor currents $i_{\text{L}1\text{d}}$ and $i_{\text{L}2\text{d}}$ are calculated via the power conservation at the equilibrium point (fixed-point). Refer to (5) and (6), one sets dx/dt = 0, x= x_{d}, and simplify $R_1 = R_2$:

$$p_{\text{FCd}}=\frac{{v_{\text{FC}}}^2}{4R_1}\left(1-\sqrt{1-\frac{8R_1(v_{\text{Cd}}\cdot i_{\text{Load}})}{{v_{\text{FC}}}^2}}\right)$$

(18)

Due to the variations and uncertainties of converter parameters, the proposed control may not be able to control the converter output voltage at the desired value exactly, resulting in a steady-state output voltage error $e_3 \neq 0$. This disadvantage has to be defeat using an integral action added to the desired input power estimation (18) as follows:

$$p_{\text{FCREF}}=p_{\text{FCd}}+K_{\text{cor}}\int\overbrace{(v_{\text{Cd}}-v_{\text{C}})}^{e_3}\cdot dt$$

(19)

where K_{cor} is the integral gain. This results

$$i_{\text{L}1\text{d}}=i_{\text{L}2\text{d}}=\left(\frac{p_{\text{FCREF}}}{v_{\text{FC}}}\right)\Big/2.$$

(20)

D. Controller Design

Refer to (3) and substituting (16) and (17) into (9), the state variables can be written as below

$$i_{\text{L}1}=\int_{t_0}^{t}\left(\frac{R_1}{L_1}e_1+K_{\text{r}1}L_1e_1+K_{\text{j}13}C_{\text{Bus}}e_3+\frac{1}{L_1}e_3\right)dt+\overbrace{I_{L1}^{ini}}$$

(21)

$$i_{\text{L}2}=\int_{t_0}^{t}\left(\frac{R_2}{L_2}e_2+K_{\text{r}2}L_2e_2+K_{\text{j}23}C_{\text{Bus}}e_3+\frac{1}{L_2}e_3\right)dt+\overbrace{I_{L2}^{ini}}$$

(22)

From the control point of view for the boost converter, the state variables $i_{\text{L}1}$ and $i_{\text{L}2}$ must be controlled to be

stronger than v_C and to adjust the damping of the system, one may set the controller gains to compensate the lumped-elements: L_1, L_2 and C_{Bus}

$$K_{r1} = \frac{K_{R1}}{L_1} > K_{j13} = \frac{K_{J13}}{C_{Bus}} > 0$$

(23)

$$K_{r2} = \frac{K_{R2}}{L_2} > K_{j23} = \frac{K_{J23}}{C_{Bus}} > 0$$

(24)

where K_{R1}, K_{R2}, K_{J13}, and K_{J13} are the damping controller gains.

E. Stability Analysis

We define the closed-loop Hamiltonian function (12) as the Lyapunov candidate function V,

$$V = \mathbf{H}_d(x)$$

(25)

The derivative of the function V can be expressed as

$$\dot{V} = \frac{d\mathbf{H}_d(x)}{dt} = \left(\frac{\partial \mathbf{H}_d(x)}{\partial x}\right)^T \frac{dx}{dt}$$

$$= -\left(\frac{\partial \mathbf{H}_d(x)}{\partial x}\right)^T \mathbf{R}_d \frac{\partial \mathbf{H}_d(x)}{\partial x} < 0 .$$

(26)

Combining (25) and (26), we gain,

$$V > 0 , \dot{V} < 0$$

(27)

For this reason, $H_d(x)$ can be qualified as a Lyapunov function; the stability of the equilibrium point is ensured.

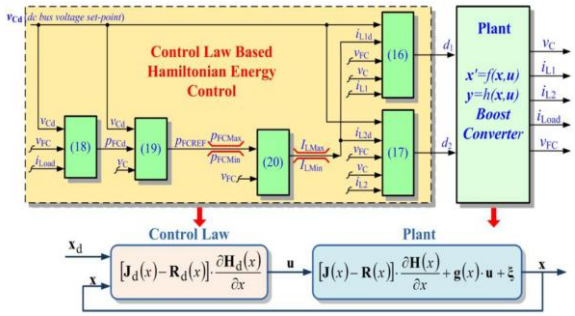


Fig. 3. Proposed passivity control scheme based on the port-controlled Hamiltonian for the multiphase interleaved FC boost converter.

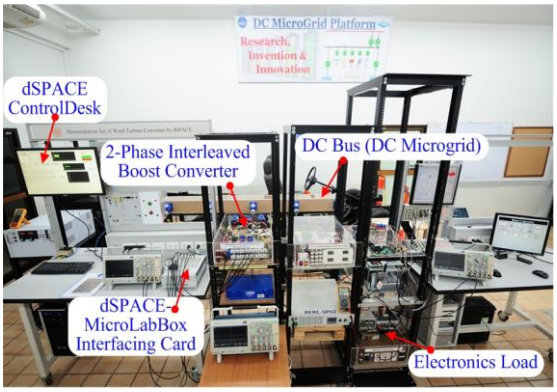


Fig. 4. Test bench system of dc microgrid platform at the Renewable Energy Research Centre (RERC).



Fig. 5. Test bench of PEMFC/Reformer System of 2.5 W, 50 V.

Symbol	Quantity	Nominal Value
v_{FC}	Input fuel cell voltage	50 V
v_{Cd}	DC bus voltage reference	100 V
L_1	1st Inductance	187 µH
L_2	2nd Inductance	170 µH
$R_1 = R_2$	Equipvalent serial resistances	0.06 Ω
C_{Bus}	Total DC bus capacitance	2,000 µH
f_S	Switching Frequency	25 kHz

TABLE I. 2-Phase FC Boost Converter

Symbol	Value	Symbol	Value
K_{R1}	21,390	K_{R2}	21,390
K_{J13}	20,695	K_{J23}	20,695
K_{cor}	400	P_{FCMax}	1.5 kW
I_{LMax}	15 A		

TABLE II. Controller Parameters

F. Conclusion of the Control Law

The multivariable control of the FC converter previously detailed is depicted in Fig. 3. Equation (19) generates a FC power reference p_{FCREF}. For safety, p_{FCREF} must be limited in level, i.e., within an interval [maximum FC power p_{FCMax} (corresponding to a FC rated power), minimum FC power p_{FCMin} (set to 0 W)]. Then, equation (20) generates an inductor current command $i_{Ld} = i_{L1d} = i_{L2d}$. For safety again, i_{Ld} must be limited in level, i.e., within an interval [maximum inductor current i_{LMax} (corresponding to a FC rated current x 50%), minimum inductor current i_{LMin} (set to 0 A)]. Finally, equations (16) and (17) generate duty cycle control signals d_1 and d_2.

III. PERFORMANCE VALIDATION

The test bench of the studied dc microgrid was realized in the laboratory, as shown in Fig. 4, with the prototype FC converter of 2.5 kW implemented in the Renewable Energy Research Centre (RERC). The converter parameters are presented in Table I. The FC system (based on H2 PowerTech LLC) used in this effort was a PEMFC system (2.5 kW, 50 V), as displayed in Fig. 5. The Methanol PEMFC system includes a fuel reformer (see Fig. 1) that converts methanol and water liquid fuel into hydrogen gas to FC stack. The parameters associated with the Hamiltonian control law are summarized in Table II.

The control law (see Fig. 4) was implemented in the real-time card dSPACE MicroLabBox platform (see Fig. 4) with a sampling time of 40 μs (25 kHz, which is equal to the power switching frequency f_s of the converter in Table I), through the mathematical environment of MATLAB–Simulink. The experimental tests were operated by connecting a dc microgrid of 100 V loaded by an electronic load.

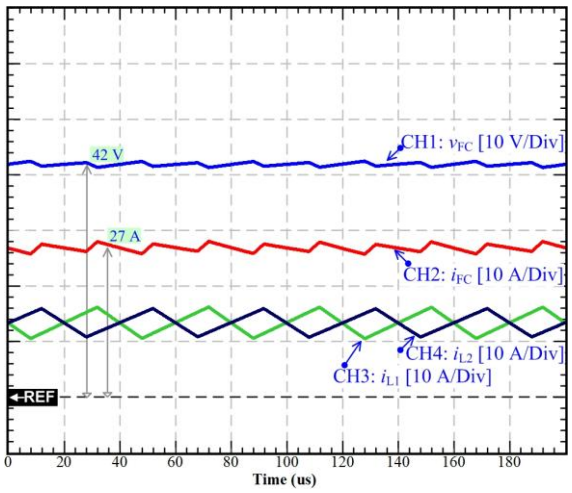


Fig. 6. Simulation results: Equilibrium point waveforms of the FC converter at $v_{Cd} = v_C = 100$ V and $p_{Load} \approx p_{FC} = 1{,}100$ W.

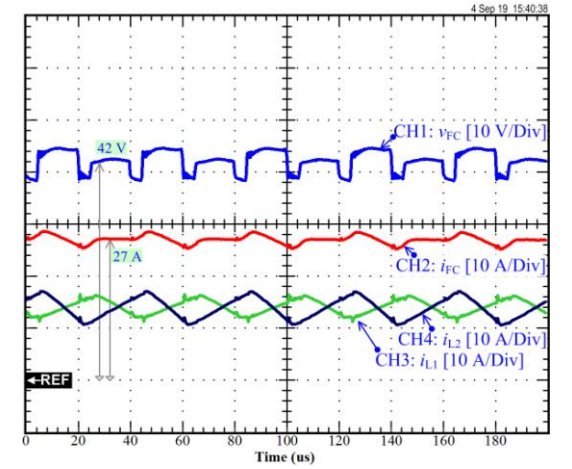


Fig. 7. Experimental results: Equilibrium point waveforms of the FC converter at $v_{Cd} = v_C = 100$ V and $p_{Load} \approx p_{FC} = 1{,}100$ W.

To validate the system modeling, the simulation was implemented. Simulations with MATLAB/Simulink were performed using a switching model of the 2-phase FC boost converter. The equilibrium point waveforms in Figs. 6 and 7 portray the characteristics of the interleaved converters at the $v_{Cd} = v_C = 100$ V and $p_{FC} \approx p_{Load} = 1{,}100$ W (CPL). The data illustrate the FC voltage, the FC current, the 1st inductor current, and the 2nd inductor current. One can observe that the paralleled interleaving-boost converter uses forced current sharing between the power stages to balance the power that the stages deliver and the FC current is the sum of the inductor currents and that the FC ripple current is 1/N the individual inductor ripple currents. So, the FC ripple current of the two-cell interleaved converter is nearly zero. The simulation results and experimantal results are closed, so that it is clear that the system modeling is corrected.

Finally, to demonstrate dc bus voltage v_C stabilization by the Hamiltonian control law, the waveforms in Fig. 8 show the response of the state variables x and the control variables u to the large load power demands (disturbance). The screens show the dc bus voltage x_3, the FC voltage, the

FC current, the load power, the 1st inductor current, the 2nd inductor current, the 1st duty cycle, and 2nd duty cycle. The experimental results in Fig. 8 present the response to a step CPL from 660 W to 840 W. The dc-bus voltage is globally asymptotically stable during the large step in a CPL and the duty cycles are moved to a new equilibrium point, which is of key significance by using the proposed Hamiltonian control law.

IV. CONCLUSION

DC microgrids often invoke the need to parallel dc/dc or ac/dc power converters for a variety of reasons, i.e., improved maintainability, enhanced reliability, distributing heat sources, and enabling the use of standardized designs with varying loads. The proposed converter is two-phase parallel step-up FC converters with the interleaved switching technique. Moreover, it is identified that a CPL connected to a dc microgrid may lead to fluctuation or even instability

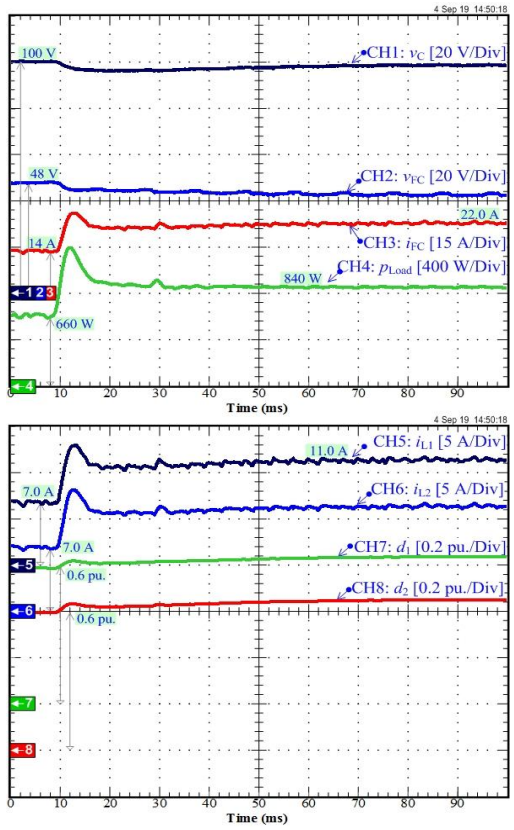


Fig. 8. Experimental results: Dynamic characteristic of the converter during a constant power load step from 660 W to 840 W.

when classic linear controllers are implemented. Then, controlling an interleaved multiphase power converter is the same as controlling a single step-up converter, but the uniqueness of the proposed method is the new control law based on the port-Hamiltonian energy control. Using the nonlinear-control approach based on the Hamiltonian Lyapunov property, we have proposed a simple solution to the stabilization and optimization problems in the nonlinear power-electronic system. This is the novel concept for this kind of application. Simulation and experimental results showed that the proposed controller has excellent performance under a CPL.

Finally, the port-controlled Hamiltonian is a model-based control approach. It requires to know system parameters (such R_1, R_2, etc.) to obtain the Hamiltonian property. For future works, some online state observers (or parameter observers) will be employed to improve the system performances.

ACKNOWLEDGMENT

This work was supported in part by the research program in cooperation under "International Research Common Laboratory" between King Mongkut's University of Technology North Bangkok and Université de Lorraine under Grant KMUTNB–GOV–60–002.

REFERENCES

[1] D. Zhou, A. Al-Durra, I.Matraji, A. Ravey, and F. Gao, "Online Energy Management Strategy of Fuel Cell Hybrid Electric Vehicles: A Fractional-Order Extremum Seeking Method," IEEE Trans. Ind. Electron., vol. 65, no. 8, pp. 6787–6799, Aug. 2018.

[2] H. Fathabadi, "Fuel cell hybrid electric vehicle (FCHEV): Novel fuel cell/SC hybrid power generation system," Energy Conversion and Management, vol. 156, pp. 192–201, Jan. 2018.

[3] N. Bizon and P. Thounthong , "Fuel economy using the global optimization of the Fuel Cell Hybrid Power Systems," Energy Conversion and Management, vol. 172, pp. 665–678, Oct. 2018.

[4] P. Thounthong, B. Davat, S. Raël, and P. Sethakul, "Fuel cell high power applications," IEEE Ind. Electron. Mag., vol. 3, no. 1, pp. 32–46, Mar. 2009.

[5] N. Bizon, P. Thounthong, M. Raducu, L. M. Constantinescu, "Designing and modelling of the asymptotic perturbed extremum seeking control scheme for tracking the global extreme," Int. J. hydrogen energy, vol. 42, pp. 17632–17644, 2017.

[6] P. Thounthong, B. Davat, S. Raël, and P. Sethakul, "Fuel starvation: Analysis of a PEM fuel cell system," IEEE Ind. Appl. Mag., vol. 15, no. 4, pp. 52–59, Jul./Aug. 2009.

[7] F. Slah, A. Mansour, M. Hajer, and B. Faouzi, "Analysis, modeling and implementation of an interleaved boost DC-DC converter for fuel cell used in electric vehicle," Int. J. Hydrogen Energy, vol. 42, no. 48, pp. 28852–28864, Nov. 2017.

[8] A. M. Rahimi and A. Emadi, "An Analytical Investigation of DC/DC Power Electronic Converters With Constant Power Loads in Vehicular Power Systems," IEEE Trans. Veh. Technol., vol. 58, no. 6, pp. 2689–2009, Jul. 2009.

[9] 9. P. Magne, D. Marx, B. Nahid-Mobarakeh, and S. Pierfederici, "Large-Signal Stabilization of a DC-Link Supplying a Constant Power Load Using a Virtual Capacitor: Impact on the Domain of Attraction," IEEE Trans. Ind. Appl., vol. 48, no. 3, pp. 878–887, May/June 2012.

[10] R. Gavagsaz-Ghoachani, L. M. Saublet, M. Phattanasak, J. Ph. Martin, B. Nahid-mobarakeh, S. Pierfederici, "Active stabilisation design of DC–DC converters with constant power load using a sampled discrete-time model: stability analysis and experimental verification," IET Power Electronics, vol. 9, pp. 1–10, 2018.

[11] M. A. Kardan, M. H. Asemani, A. Khayatian, N. Vafamand, M. H. Khooban, T. Dragicevic, and F. Blaabjerg, "Improved Stabilization of Nonlinear DC Microgrids: Cubature Kalman Filter Approach," IEEE Trans. Ind. Appl., vol. 54, no. 5, pp. 5104–5112, Sep./Oct. 2018.

[12] O. D. Montoya, W. Gil-González, and F. M. Serra, "PBC Approach for SMES Devices in Electric Distribution Networks," IEEE Trans. Circuits Syst. II, Exp. Briefs, vol. 65, no. 12, pp. 2003–2007, Dec. 2018.

[13] M. Zhang, P. Borja, R. Ortega, Z. Liu, and H. Su, "PID Passivity-Based Control of Port-Hamiltonian Systems," IEEE Trans. Automat. Control, vol. 63, no. 4, pp. 1032–1044, Apr. 2018.

[14] Z. Liu, Z. Geng, and X. Hu, "An Approach to Suppress Low Frequency Oscillation in the Traction Network of High-Speed Railway Using Passivity-Based Control," IEEE Trans. Power Syst., vol. 33, no. 4, pp. 3909–3918, July 2018.

[15] Y. Lei, X. Lin, and Y. Zhu, "Passivity-Based Control Strategy for SMES Under an Unbalanced Voltage Condition," IEEE Access, vol. 6, pp. 28768–28776, 2018.

[16] B. Fu, Q. Wang and W. He, "Nonlinear Disturbance Observer-Based Control for a Class of Port-Controlled Hamiltonian Disturbed Systems ," IEEE Access, vol. 6, pp. 50299–50305, 2018.

[17] P. Thounthong and B. Davat, "Study of a multiphase interleaved step-up converter for fuel cell high power applications,," Energy Convers. Manage., vol. 51, no. 4, pp. 826–832, Apr. 2010.

[18] P. Thounthong and S. Pierfederici, "A new control law based on the differential flatness principle for multiphase interleaved DC–DC converter," IEEE Trans. Circuits Syst. II, Exp. Briefs, vol. 57, no. 11, pp. 903–907, Nov. 2010.

★★★